



## Design, synthesis and biological evaluation of a novel series of anthrapyrazoles linked with netropsin-like oligopyrrole carboxamides as anticancer agents

Rui Zhang<sup>a</sup>, Xing Wu<sup>a</sup>, Lynn J. Guzic<sup>b</sup>, Frank S. Guzic<sup>b</sup>, Gaik-Lean Chee<sup>a</sup>, Jack C. Yalowich<sup>c</sup>, Brian B. Hasinoff<sup>a,\*</sup>

<sup>a</sup> Faculty of Pharmacy, 750 McDermot Avenue, University of Manitoba, Winnipeg, Manitoba, Canada R3E 0T5

<sup>b</sup> Department of Chemistry and Biochemistry, Southwestern University, Georgetown, TX 78628, USA

<sup>c</sup> Department of Pharmacology and Chemical Biology, University of Pittsburgh School of Medicine, Pittsburgh, PA 15261, USA

### ARTICLE INFO

#### Article history:

Received 8 February 2010

Revised 7 April 2010

Accepted 9 April 2010

Available online 18 April 2010

#### Keywords:

Netropsin

DNA

Minor groove

Intercalator

Anthrapyrazole

Anticancer

Topoisomerase I

Topoisomerase II

Cytotoxic

### ABSTRACT

Anticancer drugs that bind to DNA and inhibit DNA-processing enzymes represent an important class of anticancer drugs. Combilexin molecules, which combine DNA minor groove binding and intercalating functionalities, have the potential for increased DNA binding affinity and increased selectivity due to their dual mode of DNA binding. This study describes the synthesis of DNA minor groove binder netropsin analogs containing either one or two *N*-methylpyrrole carboxamide groups linked to DNA-intercalating anthrapyrazoles. Those hybrid molecules which had both two *N*-methylpyrrole groups and terminal (dimethylamino)alkyl side chains displayed submicromolar cytotoxicity towards K562 human leukemia cells. The combilexins were also evaluated for DNA binding by measuring the increase in DNA melting temperature, for DNA topoisomerase II $\alpha$ -mediated double strand cleavage of DNA, for inhibition of DNA topoisomerase II $\alpha$  decatenation activity, and for inhibition of DNA topoisomerase I relaxation of DNA. Several of the compounds stabilized the DNA–topoisomerase II $\alpha$  covalent complex indicating that they acted as topoisomerase II $\alpha$  poisons. Some of the combilexins had higher affinity for DNA than their parent anthrapyrazoles. In conclusion, a novel group of compounds combining DNA intercalating anthrapyrazole groups and minor groove binding netropsin analogs have been designed, synthesized and biologically evaluated as possible novel anticancer agents.

© 2010 Elsevier Ltd. All rights reserved.

### 1. Introduction

Anticancer drugs such as doxorubicin, daunorubicin, amsacrine and mitoxantrone are planar molecules that intercalate into DNA and in doing so inhibit DNA topoisomerase II (EC 5.99.1.3) and cause DNA strand breaks which results in cell growth inhibition and/or cell death.<sup>1</sup> The anthracyclines doxorubicin and daunorubicin are quinones and can be reductively activated to form reactive oxygen species.<sup>2</sup> It is the oxidative stress on the relatively unprotected cardiac muscle that likely leads to a cumulative dose-dependent and potentially fatal cardiotoxicity. The anthrapyrazoles, while sharing some of the DNA binding structural features of the anthracyclines, cannot, however, be reductively activated because they are not quinones. As such they are not likely to be cardiotoxic. In previous studies, we designed, synthesized and tested several classes of anthrapyrazole analogs of loxoxantrone and piroxantrone<sup>3,4</sup> that exhibited potent cancer cell growth inhibitory effects.<sup>5–7</sup> These anthrapyrazole analogs included both monointercalating<sup>5</sup> and bisintercalating<sup>6,7</sup> compounds. Compounds most

commonly bind to DNA by intercalating between the DNA base pairs or by binding in the DNA minor groove. Natural products such as netropsin (**1**) and distamycin A (**2**) (Fig. 1) are crescent-shaped molecules that contain an oligopyrrole carboxamide chain and cationic end side chains that result in very high affinity for AT-rich sequences of DNA.<sup>8–10</sup> In principle, hybrid molecules that contain both intercalating and minor groove binding functionalities should be able to interact more strongly with DNA than either individual functionality, and thus should have a prolonged residence time on DNA allowing them to interfere with DNA processing enzymes.<sup>9,11–13</sup> These hybrid molecules, because of their dual binding mode of action, have been called combilexins and are composed of (1) intercalators based on analogs of amsacrine, ellipticine, anthraquinones and mitoxantrone and (2) minor groove binders based on analogs of netropsin or distamycin A.<sup>8,11–13</sup> Combilexins should, in principle, also have enhanced DNA sequence specificity compared to monointercalators or minor groove binders. In this study, we have designed, synthesized and tested a series of combilexins (Figs. 1 and 2) based on the DNA-intercalating anthrapyrazoles and the DNA minor groove binding netropsin. In addition to measuring the cell growth inhibitory effects of these compounds, we also measured their ability to bind to DNA, to

\* Corresponding author. Tel.: +1 204 474 8325; fax: +1 204 474 7617.

E-mail address: [B\\_Hasinoff@UManitoba.ca](mailto:B_Hasinoff@UManitoba.ca) (B.B. Hasinoff).

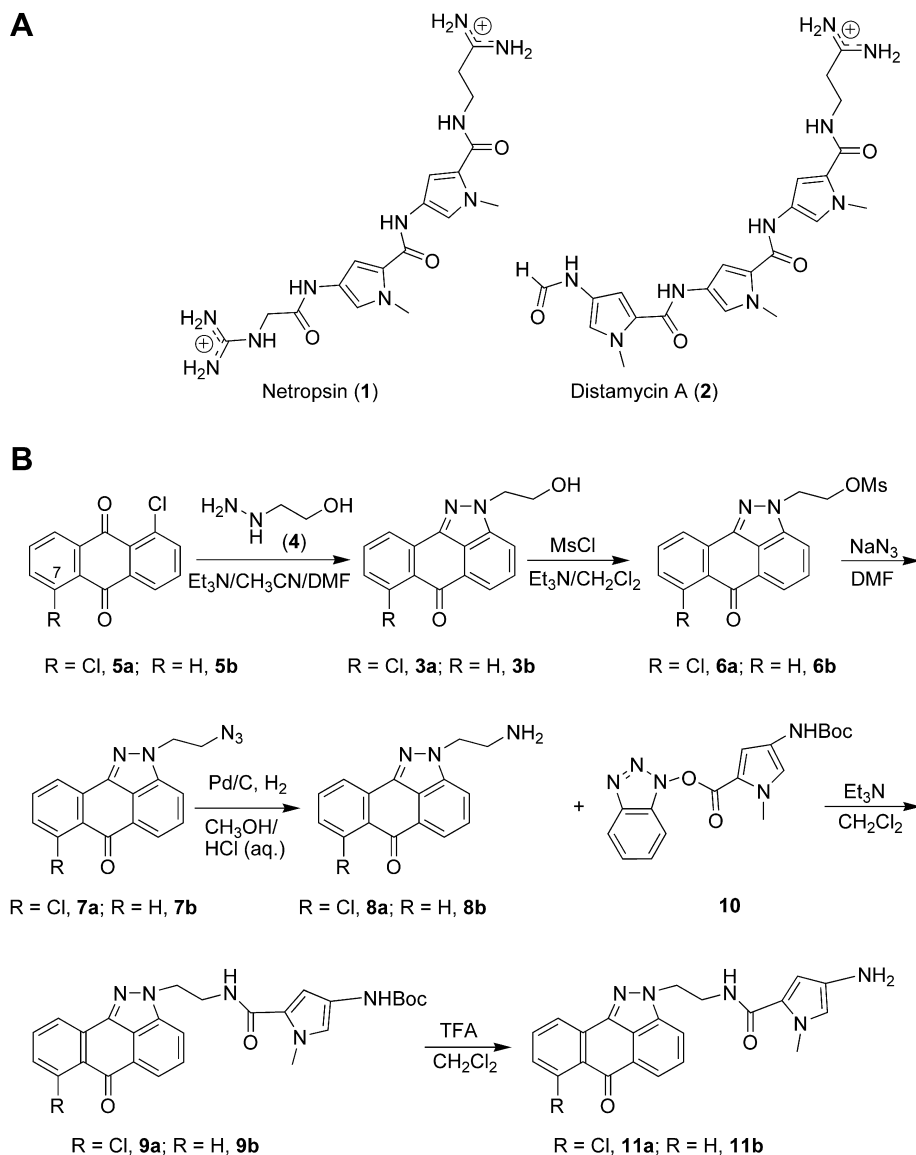


**Figure 1.** (A) Netropsin (**1**) and distamycin (**2**). (B) Reaction scheme and structures for the synthesis of the precursors and the intermediates for the preparation of the anthrapyrazole-netropsin combilexin compounds.

inhibit topoisomerase I, topoisomerase II $\alpha$ , and to cause topoisomerase II $\alpha$ -mediated DNA cleavage.

## 2. Results

### 2.1. Synthesis of the anthrapyrazole-netropsin analogs

The intercalator anthrapyrazoles **3**, and **6–8**, and the anthrapyrazole-netropsin combilexins **9**, and **11–16** were synthesized as shown in **Figures 1B** and **2**. There were two series of analogs, **a** and **b**, prepared for each compound class with the exception of **16**. The analogs in series **a** consist of a chloro substituent at the 7-position, whereas the analogs in series **b** are unsubstituted at that position. The first intermediates, anthrapyrazole alcohols **3**, were prepared in 75–80% yields via condensation of commercially available anthraquinones **5** with hydrazine **4**. The subsequent conversion of the alcohols **3** into the amines **8** were carried out in three steps via mesylation, azidation, and hydrogenation in low to moderate overall yields. The amines **8** underwent smooth coupling with the *N*-methylpyrrole acylating agent **10** in the presence of triethylamine to afford the *t*-Boc protected anthrapyrazole-netropsin

analog **9**. Removal of the *t*-Boc protecting group under acidic condition gave the amino *N*-methylpyrrole **11** quantitatively as common precursors to the other series of combilexins. Introduction of the (dimethylamino)acetyl group onto **11** via acylation occurred efficiently to give **12**. On the other hand, reacting **11** with the acylating agent **10** afforded *N*-methylpyrrole dimers **13** that mimicked netropsin more closely. Deprotection of the *t*-Boc group from **13** followed by introduction of the (dimethylamino)acetyl group using the same methods described above yielded **15** in good overall yields. The final analog that contained two (dimethylamino)alkyl side chains at both ends of the molecule, **16**, was prepared from **15a** by replacing the 7-chloro substituent with (dimethylamino)ethylamine in heated DMSO. The reaction did not proceed cleanly, affording analog **16** in only 20% yield after chromatography.

### 2.2. Effect of the anthrapyrazole-netropsin analogs on the thermal denaturation of DNA

**Table 1** shows the increase in DNA melting temperature,  $\Delta T_m$ , of sonicated calf thymus DNA (5  $\mu$ g/mL), induced by 1  $\mu$ M of the anthrapyrazole-netropsin combilexin compounds and some of

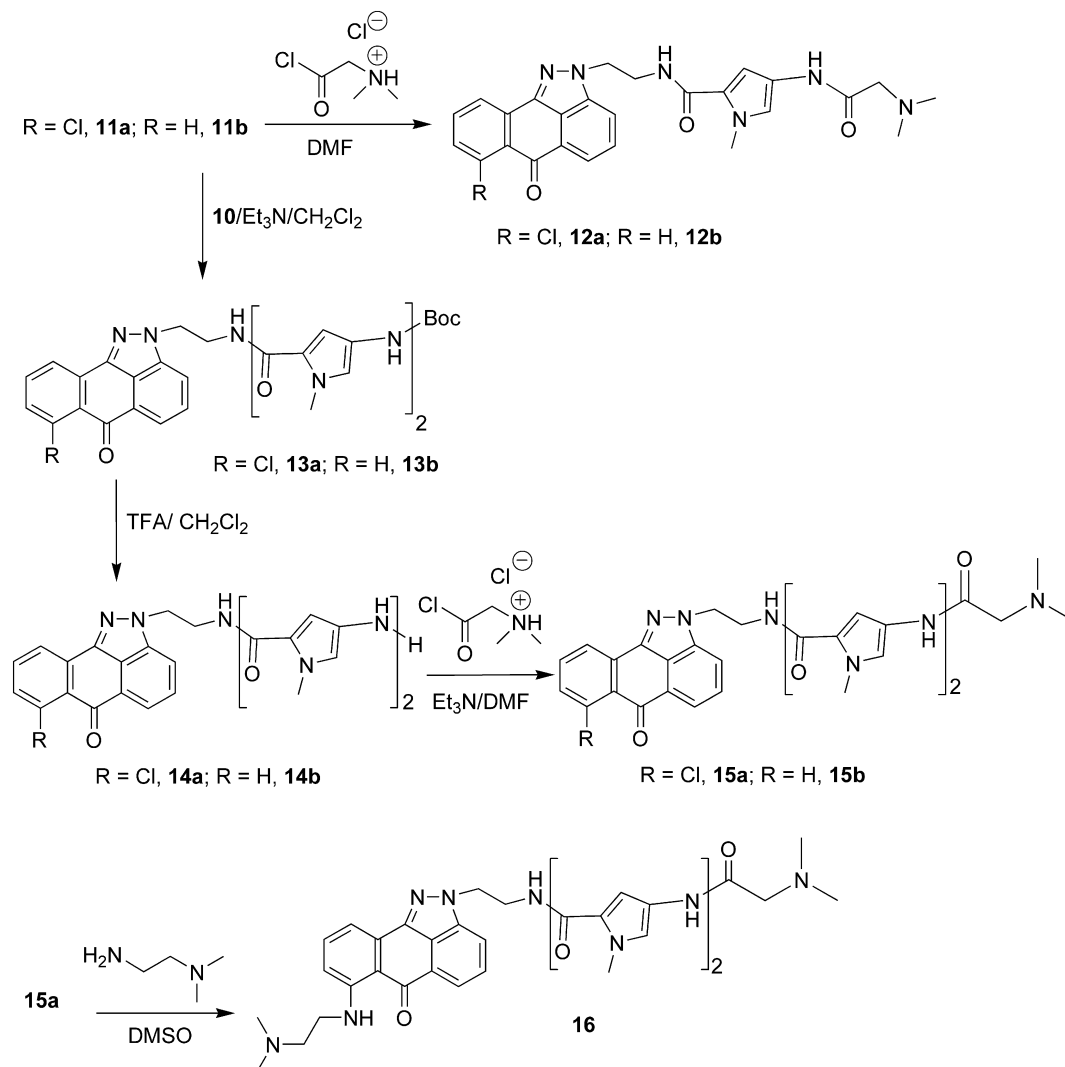


**Figure 2.** Reaction scheme and structures for the synthesis of the anthrapyrazole-netropsin combilexin compounds.

their precursors. None of the compounds tested, including netropsin itself, increased  $T_m$  as much as the positive control, the strong DNA intercalator doxorubicin, which increased  $T_m$  by 8.4 °C. The compound that increased  $T_m$  the most ( $\Delta T_m$  of 5.3 °C) was the anthrapyrazole-netropsin **16** which contained two *N*-methylpyrrole groups with two (dimethylamino)alkyl side chains at both ends of the molecule. Both of these dimethylamines would be partially protonated at biological pH which should result in an enhanced electrostatic interaction with the anionic DNA. Compound **15b**, which is a close analog of **16**, but which lacks the (dimethylamino)alkyl side chain substituted at the 7-position of the anthrapyrazole, increased the DNA melting temperature ( $\Delta T_m$  of 4.3 °C) just slightly less than **15b**. Compound **15a**, which is the 7-chloro analog of **15b**, increased  $T_m$  by only 1.7 °C, suggesting that the molecule containing a chloro group decreased DNA binding possibly because its increased size interfered with intercalation. This was also true of the **3a/3b**, **11a/11b**, **12a/12b** pairs. In general, as exemplified by the **15a/14a/13a** and the **15b/14b/13b** sets, compounds in these sets with (dimethylamino)alkyl side chains bound stronger to DNA than did those with 4-amino-*N*-methylpyrrole terminal groups, and those in turn bound stronger than those containing bulky terminal *tert*-butoxyl side chains. The strong DNA binding of **15b** and **16** was likely due to protonation of their (dimethylamino)alkyl side chains. Under the conditions of the assay,

compounds with 4-amino-*N*-methylpyrrole terminal groups such as **14a** and **14b** would not be protonated. Also, as exemplified by the **15a/12a** and **15b/12b** pairs, compounds with two *N*-methylpyrrole groups bound DNA more strongly than those with one *N*-methylpyrrole group. This latter result suggests that the compounds with two *N*-methylpyrrole groups interacted more strongly with DNA in the minor groove. Netropsin itself increased  $T_m$  by 5.7 °C. Of the anthrapyrazole-netropsin compounds synthesized only compound **16** approached this value which suggests that the addition of the anthrapyrazole moiety did not increase strength of DNA binding.

### 2.3. Effect of the anthrapyrazole-netropsin compounds on the inhibition of the relaxation activity of topoisomerase I, the decatenation activity of topoisomerase II $\alpha$ and on the stabilization of the covalent topoisomerase II $\alpha$ -DNA cleavable complex

Experiments to determine if the compounds of Table 1 could inhibit the topoisomerase I relaxing activity of supercoiled pBR322 DNA were carried out as we previously described.<sup>14</sup> Topoisomerase I is a DNA-processing enzyme<sup>15</sup> that relieves torsional stress in DNA. Unlike topoisomerase II, topoisomerase I does not require an ATP cofactor. Topoisomerase I relaxes DNA through a transient single strand break in DNA as compared to the transient double

**Table 1**DNA binding, cell growth inhibition, topoisomerase II $\alpha$  and topoisomerase I inhibitory effects of the anthrapyrazoles

Compound	$\Delta T_m^a$ (°C)	MTS cell growth inhibition		Resistance factor <sup>b</sup>	Topoisomerase II $\alpha$		Topoisomerase I
		K562 IC <sub>50</sub> ( $\mu$ M)	K/VP.5 IC <sub>50</sub> ( $\mu$ M)		% inhibition <sup>c</sup>	% cleavage <sup>d</sup>	
<b>3a</b>	0.3	14.3	12.0	0.8	56	14	70
<b>3b</b>	0.9	11.9	10.2	0.9	60	24	66
<b>8a</b>	2.7	3.3	3.5	1.0	100	18	62
<b>8b</b>	2.2	1.8	3.1	1.7	75	29	100
<b>9a</b>	0.7	10.7	11.0	1.0	94	11	47
<b>9b</b>	1.3	14.4	22.0	1.5	91	18	11
<b>11a</b>	0.8	9.9	11.4	1.2	91	29	14
<b>11b</b>	1.8	12.7	21.9	1.7	94	26	10
<b>12a</b>	0.6	3.5	5.3	1.5	97	22	21
<b>12b</b>	1.6	2.7	3.9	1.4	94	18	16
<b>13a</b>	1.0	2.0	1.4	0.7	97	24	47
<b>13b</b>	0.4	1.0	0.82	0.8	91	4	31
<b>14a</b>	0.6	12.5	36.6	2.9	94	16	52
<b>14b</b>	2.7	4.1	6.4	1.5	91	6	49
<b>15a</b>	1.7	0.19	0.21	1.1	97	ND	31
<b>15b</b>	4.3	0.13	0.14	1.1	91	ND	23
<b>16</b>	5.3	0.21	0.63	3.0	ND	ND	ND
Netropsin	5.7	>50	>50	ND	39	0	ND
Doxorubicin	8.4	0.033	0.52	15.9	30	0	ND

<sup>a</sup> Least squares calculated best fit value at 1  $\mu$ M.<sup>b</sup> The resistance factor was calculated from the ratio of the IC<sub>50</sub> value for the K/VP.5 cell line divided by that for the K562 cell line. ND is not determined. It was not possible to evaluate the topoisomerase I or topoisomerase II inhibitory or cleavage activity of **16** because it greatly reduced the fluorescence of the DNA–ethidium bromide complex. Because of band shifting and broadening the % cleavage of **15a** and **15b** could not be determined.<sup>c</sup> At 20  $\mu$ M.<sup>d</sup> At 100  $\mu$ M.<sup>e</sup> At 20  $\mu$ M.

strand break in DNA induced by topoisomerase II.<sup>15</sup> As shown by the gel image in Figure 3, at 20  $\mu$ M most of the compounds detectably inhibited the relaxation activity of topoisomerase I towards supercoiled pBR322 DNA. The well known topoisomerase I inhibitor camptothecin at 50  $\mu$ M was used as a positive control.<sup>15</sup> The percentage inhibition results obtained from densitometry are shown in Table 1 and the values ranged from 10% to 100% inhibition.

Torsional stress that occurs in DNA during replication and transcription and daughter strand separation during mitosis is relieved by topoisomerase II which alters DNA topology by catalyzing the passing of an intact DNA double helix through a transient double-stranded break made in a second helix.<sup>16,17</sup> The ability of 20  $\mu$ M of the compounds to inhibit the decatenation of concatenated kDNA by topoisomerase II $\alpha$  was determined as previously described.<sup>18</sup> Densitometry of fully decatenated open circular DNA band in the gel image of Figure 4A was used to calculate the percentage inhibition data of Table 1. As shown in Table 1 all of the compounds strongly inhibited the decatenation activity of human topoisomerase II $\alpha$  at 20  $\mu$ M. Anthrapyrazoles **3a** and **3b** with hydroxyethyl side chains were the least effective in their inhibition of topoisomerase II $\alpha$  decatenation (Table 1). For comparison

netropsin and doxorubicin (at 20  $\mu$ M) inhibited the decatenation activity of topoisomerase II $\alpha$  by 39% and 30%, respectively. Thus, while netropsin bound DNA more strongly than the anthrapyrazole–netropsin compounds, it was not as potent an inhibitor of the decatenation activity of topoisomerase II $\alpha$ .

The decatenation assay is a measure of the ability of these compounds to inhibit the catalytic activity only, and is not a measure of whether these compounds acted as topoisomerase II poisons as do some widely used anticancer drugs such as the anthracyclines, piroxantrone, losoxantrone, mitoxantrone and etoposide.<sup>3,4,16,17</sup> These ‘so called’ topoisomerase II poisons exert their cytotoxicity through their ability to stabilize a covalent topoisomerase II–DNA intermediate (the cleavable complex). Stabilization of the covalent complex leads to double strand DNA breaks that are toxic to the cell. Thus, DNA cleavage assay experiments,<sup>19</sup> as we previously described<sup>5–7,20</sup> were carried out to see whether 100  $\mu$ M of the compounds stabilized the cleavable complex using 100  $\mu$ M etoposide as a positive control. As shown in Figure 4B the addition of etoposide (lane 20) to the reaction mixture containing topoisomerase II $\alpha$  and supercoiled pBR322 DNA induced formation of linear pBR322 DNA. Linear DNA was identified by comparison with linear pBR322 DNA produced by action of the restriction enzyme *HindIII*

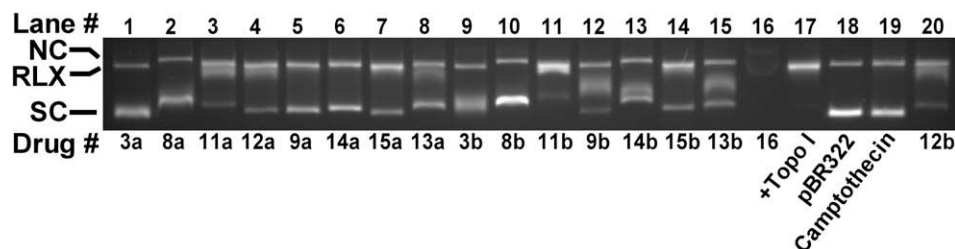


**Figure 3.** Effect of anthrapyrazole–netropsin combilexins and camptothecin on the ability of topoisomerase I to relax supercoiled pBR322 DNA. This fluorescent image of the ethidium bromide-stained gel shows that most of the compounds detectably inhibited the relaxation activity of topoisomerase I. The topoisomerase I inhibitor camptothecin (50  $\mu$ M) was used as a positive control. All lanes except lane 18 contained topoisomerase I. All drugs, where indicated, were present at a concentration of 20  $\mu$ M in the assay mixture. In this gel, which was stained with ethidium bromide after it was run, the supercoiled DNA (SC) ran ahead of the relaxed DNA (RLX). It was not possible to evaluate the topoisomerase I inhibitory activity of **16** (lane 16) because it quenched the fluorescence of the ethidium bromide–DNA complex.

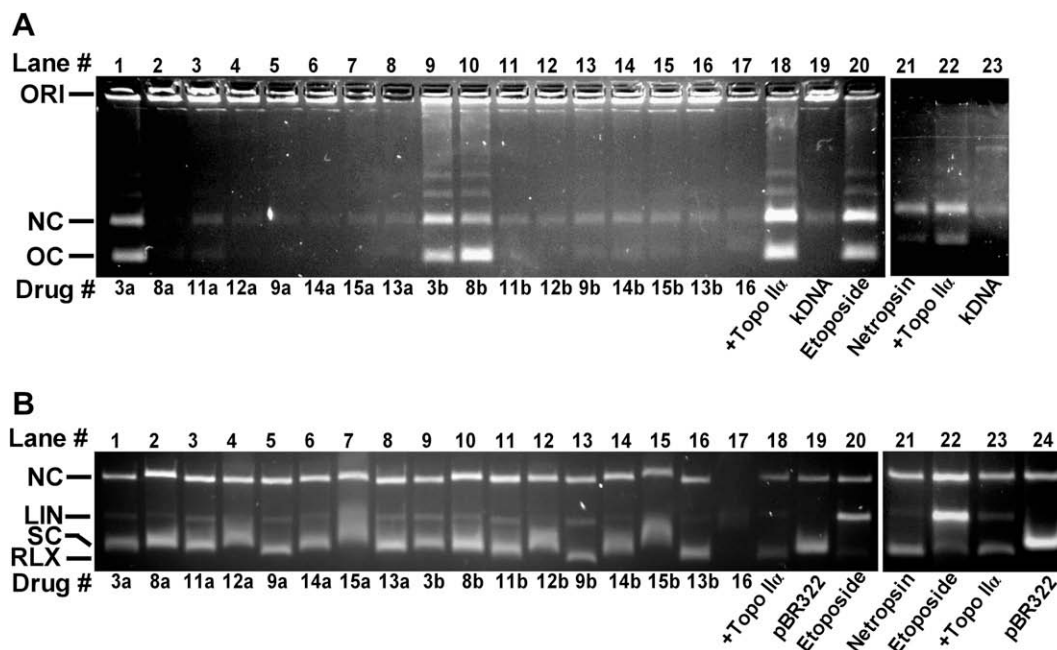


**Figure 4.** (A) Effect of anthrapyrazole–netropsin combilexins and etoposide on the topoisomerase II $\alpha$ -mediated decatenation activity of kDNA. This fluorescent image of the ethidium bromide containing gel shows that topoisomerase II $\alpha$  (Topo II $\alpha$ ) decatenated kDNA to its open circular (OC) form (lane 18). Topoisomerase II $\alpha$  was present in the reaction mixture for all lanes but lanes 19 and 23. ORI is the gel origin. All drugs, where indicated, were present at a concentration of 20  $\mu$ M in the assay mixture. Etoposide, which is only a weak catalytic inhibitor of topoisomerase II $\alpha$ , as based on densitometry inhibited the decatenation by 20%. The image in lanes 21 to 23 are from a separate gel. (B) Effect of anthrapyrazole–netropsin combilexins and etoposide on the topoisomerase II $\alpha$ -mediated relaxation and cleavage of supercoiled pBR322 plasmid DNA. This fluorescent image of the ethidium bromide-stained gel shows that topoisomerase II $\alpha$  (Topo II $\alpha$ ) converted supercoiled (SC) pBR322 DNA (lane 19) to relaxed (RLX) DNA (lane 18). In this assay the relaxed DNA runs slightly ahead of the supercoiled DNA because the gel was run in the presence of ethidium bromide. The image in lanes 21 to 24 are from a separate gel. Topoisomerase II $\alpha$  was present in the reaction mixture in all lanes but 19 and 24. As shown in lanes 20 and 22, etoposide treatment produced significant amounts of linear DNA (LIN). A small amount of nicked circular (NC) is normally present in the pBR322 DNA. A densitometric analysis of the linear DNA bands showed that all the compounds produced less linear DNA than the etoposide positive control (lanes 20 and 22). The concentration of all test compounds in the cleavage assay mixture was 100  $\mu$ M. As in the result shown in Fig. 3 it was not possible to evaluate the topoisomerase II inhibitory or cleavage activity of **16** (lane 17) because it quenched the fluorescence of the ethidium bromide–DNA complex.

acting on a single site on pBR322 DNA (not shown). Based on integrated band intensities of linear DNA in Figure 4B several of the compounds (Table 1) induced formation of linear DNA, though none were comparable (range 4–29% relative to etoposide at 100%) to that induced by etoposide in lanes 20 and 22, respectively. It was not possible to reliably quantitate the linear DNA band for either compound **15a** and **15b** (lanes 7 and 15) due to smearing of the band in this region. For comparison neither netropsin nor doxorubicin detectably induced formation of linear DNA.

It was not possible to evaluate the effects of **16** on topoisomerase I and topoisomerase II because **16** quenched the fluorescence of the ethidium bromide–DNA complex (Figs. 3 and 4). Destaining of the gel overnight in water did not solve this problem. The ability of **16** to quench the ethidium bromide–DNA fluorescence was measured in a separate dot blot type experiment carried out in the gel imaging apparatus. Using the concentration of ethidium bromide and amount of DNA used in the gel assay, **16** was observed to quench the ethidium bromide–DNA fluorescence by 94% at 30  $\mu$ M **16**. Compound **16** may be quenching the ethidium bromide–DNA fluorescence by either displacing the ethidium bromide from the DNA or by binding to DNA and quenching the fluorescence of bound ethidium bromide.

#### 2.4. Cell growth inhibitory effects of the anthrapyrazole–netropsin compounds on human leukemia K562 cells and K/VP.5 cells with a decreased level of topoisomerase II $\alpha$

As shown in Table 1 all of the anthrapyrazole–netropsin analogs potently inhibited the growth of K562 and K/VP.5 cells in the low to submicromolar range. However, the only compounds (**15a**,

**15b**, **16**) that achieved submicromolar cell growth inhibition contained two *N*-methylpyrrole groups and at least one (dimethylamino)alkyl side chain. In general, these compounds also bound DNA the strongest as indicated by their  $\Delta T_m$  values (Table 1). Netropsin itself did not inhibit the growth of K562 cells ( $IC_{50} > 50 \mu$ M, Table 1) which is consistent with previous reports in DC-3F cells indicating that netropsin had only very weak cell growth inhibitory effects ( $IC_{50}$  3.2 mM).<sup>21</sup>

Cancer cells can acquire resistance to topoisomerase II poisons by lowering their level and/or activity of topoisomerase II.<sup>16,22</sup> We previously used<sup>5–7</sup> a 26-fold etoposide-resistant K562-derived K/VP.5 cell line that had topoisomerase II $\alpha$  and topoisomerase II $\beta$  protein levels reduced sixfold and threefold,<sup>23,24</sup> respectively, to determine if any of the compounds of this study acted as topoisomerase II poisons. If there is less topoisomerase II in the cell, fewer DNA strand breaks are produced by topoisomerase II poisons which results in reduced cytotoxicity. As shown in Table 1 most of the compounds except for **16**, which was threefold resistant, displayed little or no cross resistance to K/VP.5 cells. The value for **16** compares to a value of 1.8-fold for doxorubicin and previously determined values of 1.8-, 1.7- and 4.0-fold for the topoisomerase II poisons losoxantrone, piroxantrone and mitoxantrone, respectively.<sup>5</sup> Compound **16** bound DNA the strongest and was among the most potent of the compounds, and thus it may be exerting its potency through its ability to act as a topoisomerase II poison. The resistance factor of 2.9 for **14a** was not accurately determined due to interference from the absorbance of the compounds themselves at the higher concentrations tested. Thus, both these results and the results of the cleavage assay (Table 1, Fig. 4b) suggest that some of the anthrapyrazole–netropsin compounds



may have inhibited cell growth, in part, by acting as topoisomerase II poisons.

## 2.5. Docking of the anthrapyrazole–netropsin compounds into DNA

In order to determine possible DNA binding conformations, the anthrapyrazole–netropsin compounds were docked into two different X-ray structures of DNA. In the first instance an X-ray structure (PDB ID: 1DA9)<sup>25</sup> of two molecules of doxorubicin separated by 4 base pairs intercalated into duplex DNA was used for the docking (Fig. 5A). In this structure the planar doxorubicin molecule induces outward bulges in the base pairs directly above and below it. The docking of **16** into the 1DA9 structure revealed that both NH amide groups formed H-bonds with the DNA bases. Additionally, the anthrapyrazole part of the molecule docked with its aromatic ring co-planar with the DNA bases in a configuration similar to doxorubicin. The second X-ray structure into which the compounds were docked was a netropsin–DNA complex (PDB ID: 195D).<sup>26</sup> Somewhat surprisingly the anthrapyrazole group of **16** and the other compounds docked well and completely into the minor groove of this structure (Fig. 5B). The *N*-methylpyrrole groups of compound **16** docked such that they were closely aligned and co-planar with the *N*-methylpyrrole groups in the minor groove of the 195D X-ray structure of the netropsin–DNA complex. The only H-bond formed in this structure to DNA was to the terminal (dimethylamino)alkyl side chain on the *N*-methylpyrrole chain. No instance was found of a docked structure where the intercalating anthrapyrazole part of the anthrapyrazole–netropsin compounds was docked into the 195D X-ray structure of DNA both as an intercalator and a DNA minor groove binder. This likely occurred because the adjacent base pairs in the 195D structure (Fig. 5B) are highly co-planar and are so close that they cannot accommodate an intercalator without bulging outwards. No suitable X-ray structure for docking could be found that encom-

passed both netropsin-like minor groove binding and intercalating ligands. Thus, the two structures in Figure 5A and B represent the two possible modes of **16** binding to DNA.

## 2.6. QSAR correlation analyses of DNA binding affinity, K562 cell growth inhibition, and topoisomerase I and topoisomerase II $\alpha$ inhibition

A correlation analysis was carried out on the log K562 IC<sub>50</sub> values versus the various independent variables of Table 1. The log K562 IC<sub>50</sub> values were significantly ( $p$  of 0.003), though not highly ( $r^2$  of 0.45), correlated (Fig. 6A) with  $\Delta T_m$ . This result suggests that strength of DNA binding is, in part, responsible for the growth inhibitory activity of these compounds. Correlation analyses of the log K562 IC<sub>50</sub> values with either % topoisomerase II $\alpha$  inhibition, % topoisomerase I inhibition or % cleavage did not, however, achieve significance. The lack of correlation with the inhibition of topoisomerase II $\alpha$  poisoning activity with the log IC<sub>50</sub> does not necessarily indicate that these compounds lack activity as topoisomerase II poisons, rather only that they did not act solely as topoisomerase II poisons. The lack of correlation was generally similar to what we found for our amide- and ester-linked bisanthrapyrazoles.<sup>6,7</sup>

## 3. Discussion

A series of anthrapyrazole–netropsin combilexins were synthesized and compared for their ability to inhibit K562 and K/VP.5 cell growth. Several of the compounds (**15a**, **15b** and **16**) achieved sub-micromolar IC<sub>50</sub> values. These compounds had both two *N*-methylpyrrole groups and terminal (dimethylamino)alkyl side chains that would be protonated at physiological pH. The presence of these moieties is likely responsible for the strong binding of **15a**, **15b** and **16** to DNA. These results suggest that both electrostatic and close contact interactions with the DNA minor groove are important for activity. A previously reported series of acridine–netropsin analogs did not contain a positively charged amino terminal side chain and did not display high potency, at least compared to amsacrine.<sup>27,28</sup> In another study an amsacrine–netropsin hybrid with a positively charged amino terminal side chain was thought to contribute significantly to its ATT selectivity.<sup>8</sup>

It was not possible to evaluate **16** in any of the topoisomerase I or topoisomerase II gel assays due to quenching by **16** of the ethi-

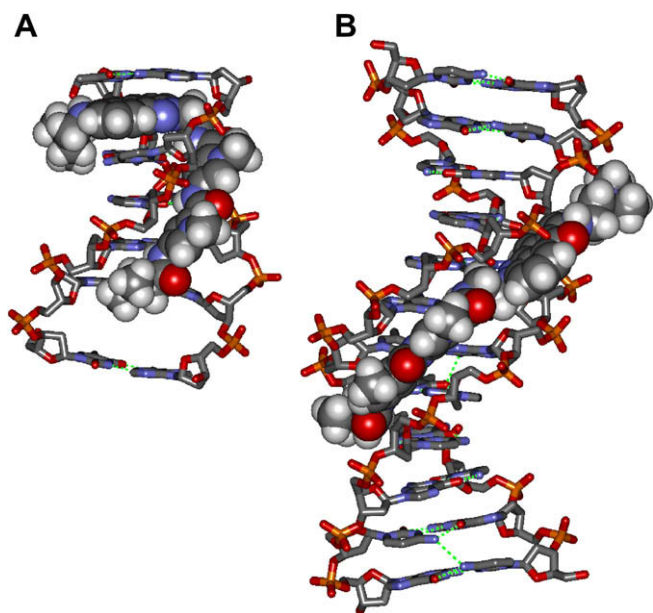


**Figure 5.** Docking of the protonated **16** compound into X-ray structures of DNA–doxorubicin and DNA–netropsin. (A) The highest scoring structure of **16** docked into the 1DA9 X-ray structure of a DNA–(doxorubicin)<sub>2</sub> complex.<sup>25</sup> (B) The highest scoring structure of **16** docked into the 195D X-ray structure of a DNA–netropsin complex in which a netropsin molecule is bound to a 12-base pair piece of DNA.<sup>26</sup> The H-atoms of the DNA are not shown for clarity. The bound ligands were removed in each case and **16** was docked into its place with the genetic algorithm docking program GOLD.

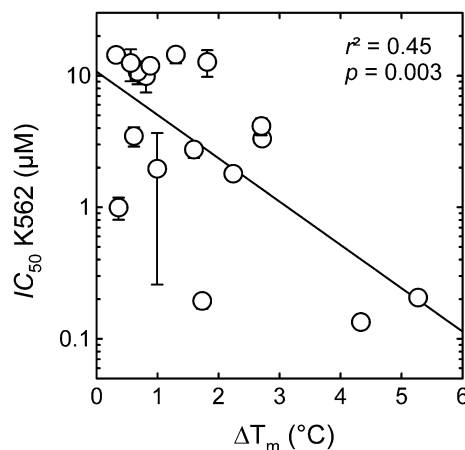


**Figure 6.** QSAR correlations of K562 cell growth inhibition and inhibition of topoisomerase II $\alpha$  decatenation activity by the anthrapyrazole–netropsin combilexins and their precursors. The log IC<sub>50</sub> values for growth inhibition and strength of DNA binding as measured by  $\Delta T_m$  were significantly correlated ( $p = 0.003$ ). The errors shown are the s.e.m.s.

dium bromide–DNA fluorescence. Netropsin itself did not, however, display any measurable cleavage activity. Compound **16**, which was among the most potent of the compounds, did, however, show the largest cross-resistance with the K/VP.5 cell line which suggests that this compound, which also bound DNA the strongest, may, in fact, also be acting as a topoisomerase II poison. Log IC<sub>50</sub> values were significantly correlated with  $\Delta T_m$  (Fig. 6), indicating that the strength of DNA binding was a reasonable predictor of cell growth inhibition. However, the strength of DNA binding was probably not the only factor that determined cell growth inhibitory activity. All of the anthrapyrazole–netropsin compounds inhibited the catalytic activity of topoisomerase I (Fig. 3) and topoisomerase II (Fig. 4A) to some degree. Because all these compounds bound to DNA to varying degrees, it is not surprising that they would interfere with the catalytic activity of these enzymes which utilize DNA as their substrate. The ability of these compounds to inhibit topoisomerase I or to stabilize topoisomerase II–DNA covalent complexes likely contributed to their cell growth inhibitory effects. Netropsin itself was a weaker inhibitor of the catalytic activity of topoisomerase II $\alpha$  than any of the anthrapyrazole–netropsin compounds.

Like some of the anthrapyrazole–netropsin combilexins several of the anthrapyrazoles and bisintercalating anthrapyrazoles we previously studied also acted as topoisomerase II $\alpha$  poisons.<sup>5–7</sup> Two anilinoacridine–netropsin hybrids (NetGA and MePyGA) were also shown by others to stabilize the topoisomerase II–DNA cleavage complex about as well as amsacrine itself.<sup>28</sup> Likewise, an ethidium–netropsin–anilinoacridine hybrid molecule (R-132) that was both an intercalator and minor groove binder stabilized the cleavage complex.<sup>13</sup> A variety of tricyclic–netropsin hybrids with terminal (dimethylamino)alkyl side chains have also been shown to have some topoisomerase II poisoning activity, in spite of the fact that they had only moderate cell growth inhibitory activity.<sup>11</sup> However, it was also found that a bis(netropsin)–anthracenedione conjugate did not stabilize the cleavage complex because the binding of the netropsin part of the molecule to DNA impeded the intercalation of the anthracenedione ring.<sup>29</sup> An amsacrine–netropsin hybrid (NetAmsa), also with two *N*-methylpyrrole groups and with a cationic terminal amino side chain, was shown to act both as an intercalator and minor groove binder,<sup>10</sup> as did an ethidium–netropsin–anilinoacridine hybrid molecule (R-132).<sup>13</sup>

The results of docking the compounds into the X-ray structures of a doxorubicin–DNA (Fig. 5A) complex or a netropsin–DNA (Fig. 5B) complex showed that the compounds could be reasonably accommodated by either structure. Thus, it was not possible to distinguish between these two possible binding modes based on the docking studies.

In summary, a series of anthrapyrazole–netropsin hybrid molecules that were designed to both intercalate and bind in the DNA minor groove were synthesized and tested for their ability to inhibit cell growth. The compounds that bound DNA the strongest and had the strongest cell growth inhibitory activity had two *N*-methylpyrrole groups and positively charged (dimethylamino)alkyl side chains which suggests that the DNA minor groove interactions were important, though not essential for activity.

## 4. Experimental

### 4.1. Biological assays

#### 4.1.1. Materials, cell culture and growth inhibition assays

The netropsin dihydrochloride was from Sigma (Oakville, Canada). The plasmid DNA and the absorbance-based cell proliferation assay and other materials were as previously described.<sup>6,7</sup> Human leukemia K562 cells, obtained from the American Type Culture Collection and K/VP.5 cells (a 26-fold etoposide-resistant K562-de-

rived sub-line with decreased levels of topoisomerase II $\alpha$  mRNA and protein)<sup>22</sup> were maintained as suspension cultures in  $\alpha$ MEM (Minimal Essential Medium Alpha, Invitrogen, Burlington, Canada) containing 10% fetal calf serum. The spectrophotometric 96-well plate cell growth inhibition 3-(4,5-dimethylthiazol-2-yl)-5-(3-carboxymethoxyphenyl)-2-(4-sulfophenyl)-2H-tetrazolium (MTS) CellTiter 96® AQueous One Solution Cell Proliferation assay Promega (Madison, WI, USA), which measures the ability of the cells to enzymatically reduce MTS after drug treatment, has been described.<sup>5</sup> The drugs were dissolved in DMSO. The final concentration of DMSO did not exceed 1.9% (v/v) and was an amount that had no detectable effect on cell growth. The cells were incubated with the drugs for 72 h and then assayed with MTS. The IC<sub>50</sub> values for cell growth inhibition were measured by fitting the absorbance–drug concentration data determined in triplicate to a four-parameter logistic equation as described.<sup>6,7</sup> As evaluated by <sup>1</sup>H NMR compound **11a** was observed to undergo extensive (80 %) decomposition to multiple products after storage in DMSO-*d*<sub>6</sub> for 24 h at room temperature. However, compounds **9a** and **9b** with their amino side chains blocked were both observed to be stable under these conditions. Thus, the assays were carried out with compounds that were dissolved in DMSO just before use.

#### 4.1.2. Topoisomerase II $\alpha$ kDNA decatenation, pBR322 DNA relaxation and cleavage assays

A gel assay as previously described<sup>18</sup> was used to determine if the compounds of Table 1 inhibited the catalytic decatenation activity of topoisomerase II $\alpha$ . kDNA, which consists of highly catenated networks of circular DNA, is decatenated by topoisomerase II $\alpha$  in an ATP-dependent reaction to yield individual minicircles of DNA. The assay conditions and the expression, extraction and purification of recombinant full-length human topoisomerase II $\alpha$  were previously described.<sup>6,7,30</sup> The percentage decatenation was obtained through densitometric analysis of the bands relative to that obtained for the fully decatenated closed circular DNA alone (arbitrarily set to 100% for the control in the absence of drug). The percentage inhibition was calculated from 100 minus the percentage relative integrated band intensity.

Topoisomerase II–cleaved DNA complexes produced by anticancer drugs may be trapped by rapidly denaturing the complexed enzyme with sodium dodecyl sulfate (SDS).<sup>5,19</sup> The drug-induced cleavage of double-stranded closed circular pBR322 DNA to form linear DNA at 37 °C was followed by separating the SDS-treated reaction products using ethidium bromide gel electrophoresis essentially as described, except that all components of the assay mixture were assembled and mixed on ice prior to addition of the drug.<sup>6,7,19</sup> The percentage cleavage was obtained through densitometric analysis of the linear DNA bands relative to that obtained for linear DNA produced by 100  $\mu$ M etoposide (arbitrarily set to 100%).

#### 4.1.3. Topoisomerase I inhibition of pBR322 DNA relaxation assay

A gel assay as previously described<sup>14</sup> was used to determine if the compounds of Table 1 inhibited topoisomerase I. The pBR322 DNA was from MBI Fermentas (Burlington, Canada). Nuclear extract, prepared as described,<sup>31</sup> was used as the source of topoisomerase I. The 20  $\mu$ L assay mixture contained 60 ng of pBR322 DNA, 50 ng of nuclear extract and 20  $\mu$ M of the test drugs. After a 20 min incubation at 37 °C in assay buffer the reaction was terminated with 0.05% (v/v) SDS. Electrophoresis was carried out as for the topoisomerase II $\alpha$  cleavage assay, except that neither the gel nor the running buffer contained ethidium bromide in order to obtain good separation of the relaxed and supercoiled DNA. In the absence of ethidium bromide the supercoiled DNA runs ahead of the relaxed DNA. The percentage inhibition was obtained

through densitometric analysis of the supercoiled bands relative to that obtained for pBR322 DNA alone (arbitrarily set to 100%) in the absence of enzyme.

#### 4.1.4. Thermal denaturation of DNA assay

Compounds that either intercalate into or bind in the minor groove of DNA stabilize the DNA double helix and increase the temperature at which the DNA denatures or unwinds.<sup>32–34</sup> The effect of 0.25, 0.5, 1.0 and 2  $\mu$ M of the compounds on the increase in melting temperature,  $\Delta T_m$ , of sonicated calf thymus DNA (5  $\mu$ g/mL) was measured in 10 mM Tris–HCl buffer (pH 7.4) in a Cary 1 (Varian, Mississauga, Canada) double beam spectrophotometer by measuring the absorbance increase at 260 nm upon the application of a temperature ramp of 1  $^{\circ}$ C/min as we previously described.<sup>5–7</sup> Doxorubicin, which is a strong DNA intercalator, was used as a positive control.<sup>5–7</sup> The least squares calculated slopes of the plot of the drug concentration versus  $\Delta T_m$  were used to calculate  $\Delta T_m$  values at a drug concentration of 1  $\mu$ M. The s.e.m.s of the slopes were typically about 0.3  $^{\circ}$ C.

## 4.2. Molecular modeling and docking

### 4.2.1. Docking of the bisanthrapyrazoles into an X-ray structure of DNA

The molecular modeling and the docking was carried out as previously described.<sup>6</sup> The protonated energy minimized forms of **8a**, **8b**, **12a**, **12b**, **15a**, **15b** and **16** that contained (dimethylamino)alkyl side chains that would be protonated at neutral pH were docked either into the doxorubicin binding site of a six-base pair X-ray crystal structure of 2 molecules of doxorubicin bound to double-stranded DNA, d(TGGCCA)/doxorubicin, ([www.rcsb.org/pdb/](http://www.rcsb.org/pdb/); PDB ID: 1DA9)<sup>25</sup> or a 12-base pair X-ray structure of a molecule of netropsin **1** (PDB ID: 195D)<sup>26</sup> bound to the minor groove of double stranded DNA, d(CGCGTTAACGCG)/netropsin, using the genetic algorithm docking program GOLD version 3.2<sup>35</sup> with default GOLD parameters and atom types and with 500 starting runs as previously described.<sup>6,7</sup> The other molecules of Table 1 were docked as their neutral forms. The two doxorubicin molecules in the 1DA9 DNA X-ray structure are separated by four intervening base pairs. The first and second base pairs buckle out to accommodate the bound doxorubicin in this structure.<sup>25</sup> The DNA structures were prepared by removing the doxorubicin or netropsin molecules and the water molecules to avoid potential interference with the docking. Hydrogens were added to the DNA with the SYBYL Biopolymer module.<sup>36</sup> The binding site (6 Å radius) was defined using a previously docked amide-linked bisanthrapyrazole that docked both intercalated and in the minor groove<sup>7</sup> for the 1DA9 structure or netropsin in the 195D structure. Doxorubicin and netropsin docked back into their respective DNA structures with a heavy atom root-mean-squared distance of 1.3 Å and 0.32 Å, respectively, compared to their X-ray structures.<sup>25,26</sup> Values of 2.0 Å or less in the extensive GOLD test set are considered to be good.<sup>37</sup> The graphic was prepared with ds Visualizer 2.0 (Accelrys, San Diego, CA). All the anthrapyrazole–netropsin compounds in Table 1 were docked into the DNA minor groove.

## 4.3. Chemistry

### 4.3.1. General

The *N*-methylpyrrolebuilding block **10** was from Oakwood Products (West Columbia, SC, USA) and dimethylaminoacetyl chloride hydrochloride was from Alfa Aesar (Ward Hill, MA, USA). Other chemicals were from Aldrich (Oakville, Canada). <sup>1</sup>H and <sup>13</sup>C nuclear magnetic resonance (NMR) spectra were recorded at 300 K in 5 mm NMR tubes on a Bruker Avance 300 MHz NMR

spectrometer operating at 300.13 MHz for <sup>1</sup>H NMR and 75.5 MHz for <sup>13</sup>C NMR, respectively, in dimethyl sulfoxide-*d*<sub>6</sub> (DMSO-*d*<sub>6</sub>), unless otherwise indicated. Chemical shifts are given in parts per million (ppm) ( $\pm 0.01$  ppm) relative to tetramethylsilane (0.00 ppm) in the case of the <sup>1</sup>H NMR spectra, and to the central line of CDCl<sub>3</sub> ( $\delta$  77.0) for the <sup>13</sup>C NMR spectra. Melting points were taken on a Gallenkamp (Loughborough, England) melting point apparatus and were uncorrected. The high resolution mass spectra were run on an Agilent 6210 Accurate-Mass Time-of-Flight LC/MS system (Agilent Technologies, Mississauga, Canada) using electrospray ionization. The samples were dissolved in methanol and were infused into the mass spectrometer with an Agilent 1200 HPLC using acetonitrile/water containing 0.1% (v/v) formic acid as the mobile phase. TLC was performed on plastic-backed plates bearing 200  $\mu$ m silica gel 60 F<sub>254</sub> (Silicycle, Quebec City, Canada). Compounds were visualized by quenching of fluorescence by UV light (254 nm) where applicable. The reaction conditions were not optimized for reaction yields. Dichloromethane and triethylamine were refluxed over calcium hydride and distilled. *N,N*-Dimethylformamide (DMF) was dried over calcium hydride and distilled under reduced pressure.

### 4.3.2. 7-Chloro-2-(2-hydroxyethyl)anthra[1,9-*cd*]pyrazol-6(2H)-one (**3a**)

2-Hydrazinoethanol (**4**) (5.2 g, 77 mmol) was added to a suspension of the dichloroanthraquinone (**5a**) (6.92 g, 25 mmol) in acetonitrile (120 mL) and DMF (10 mL). Triethylamine (4.0 mL) was then added and the mixture was heated to reflux for 60 h. The mixture was cooled to room temperature and placed in a freezer overnight. The resulting crystals were filtered, washed twice with cooled acetonitrile and dried to afford **3a** as orange crystals (5.6 g, 76%); mp: 191–192  $^{\circ}$ C; <sup>1</sup>H NMR (CDCl<sub>3</sub>)  $\delta$  8.13–8.19 (m, 1H), 7.96 (d, *J* = 6.7 Hz, 1H), 7.71–7.74 (m, 2H), 7.51–7.57 (m, 2H), 4.64 (t, *J* = 4.7 Hz, 2H), 4.21–4.26 (m, 2H), 2.74 (t, *J* = 5.9 Hz, 1H); <sup>13</sup>C NMR (CDCl<sub>3</sub>)  $\delta$  182.56, 139.66, 139.22, 138.69, 137.32, 134.42, 133.00, 132.82, 128.98, 126.95, 122.54, 121.85, 121.24, 114.88, 62.09, 51.98; HRMS (ESI), *m/z* (M+H)<sup>+</sup>: calcd 299.0582, obsd 299.0593.

### 4.3.3. 2-(2-Hydroxyethyl)anthra[1,9-*cd*]pyrazol-6(2H)-one (**3b**)

Compound **3b** was made using the same procedure as for **3a** but 1-chloroanthraquinone (**5b**) was used instead of **5a**. The reaction yielded orange crystals in 80% yield; mp: 183–185  $^{\circ}$ C; <sup>1</sup>H NMR (CDCl<sub>3</sub>)  $\delta$  8.35 (dd, *J*<sub>1</sub> = 7.9 Hz, *J*<sub>2</sub> = 1.3 Hz, 1H), 8.09 (d, *J* = 7.9 Hz, 1H), 7.87 (d, *J* = 7.0 Hz, 1H), 7.72–7.63 (m, 2H), 7.51–7.58 (m, 2H), 4.63 (t, *J* = 4.8 Hz, 2H), 4.26 (br, 2H), 3.12 (br, 1H); <sup>13</sup>C NMR (CDCl<sub>3</sub>)  $\delta$  183.52, 139.68, 139.13, 133.26, 133.09, 131.45, 129.09, 128.51, 128.40, 126.07, 123.15, 122.64, 120.91, 115.16; HRMS (ESI), *m/z* (M+H)<sup>+</sup>: calcd 265.0972, obsd 265.0981.

### 4.3.4. 7-Chloro-2-(2-methanesulfonyloxyethyl)anthra[1,9-*cd*]pyrazol-6(2H)-one (**6a**)

A suspension of **3a** (4.40 g, 14.7 mmol) and triethylamine (3.81 mL, 27.9 mmol) in dichloromethane (45 mL) was cooled to 0  $^{\circ}$ C and treated with mesyl chloride (2.00 mL, 26.0 mmol). The mixture was stirred overnight at 0  $^{\circ}$ C and then filtered. The solid obtained was washed with a large amount of water to neutrality and dried to afford **6a** as an orange solid (4.9 g, 90%); mp: 195–196  $^{\circ}$ C; <sup>1</sup>H NMR (CDCl<sub>3</sub>)  $\delta$  8.16–8.22 (m, 1H), 8.03 (dd, *J*<sub>1</sub> = 6.9 Hz, *J*<sub>2</sub> = 1.3 Hz, 1H), 7.67–7.78 (m, 2H), 7.55–7.60 (m, 2H), 4.86 (m, 2H), 4.78 (m, 2H), 2.81 (s, 3H); <sup>13</sup>C NMR (CDCl<sub>3</sub>)  $\delta$  182.46, 139.87, 139.47, 137.42, 133.08, 129.31, 127.09, 122.84, 121.90, 121.38, 114.68, 67.66, 49.20, 37.56; HRMS (ESI), *m/z* (M+H)<sup>+</sup>: calcd 377.0357, obsd 377.0372.



**4.3.5. 2-(2-Methanesulfonyloxyethyl)anthra[1,9-*cd*]pyrazol-6(2H)-one (6b)**

Using the same procedure as for **6a**, compound **6b** was prepared from **3b** to give orange crystals in 80% yield; mp: 185–187 °C; <sup>1</sup>H NMR (CDCl<sub>3</sub>) δ 8.45 (dd, *J*<sub>1</sub> = 7.9 Hz, *J*<sub>2</sub> = 1.3 Hz, 1H), 8.19 (d, *J* = 7.9 Hz, 1H), 8.06 (d, *J* = 7.0 Hz, 1H), 7.70–7.78 (m, 3H), 7.57–7.60 (m, 1H), 4.85 (t, *J* = 4.8 Hz, 2H), 4.78 (m, 2H), 2.79 (s, 3H); <sup>13</sup>C NMR (CDCl<sub>3</sub>) δ 183.50, 140.08, 139.94, 133.45, 133.37, 131.38, 129.31, 128.98, 128.79, 126.50, 123.64, 122.76, 121.11, 67.82, 49.03, 37.50; HRMS (ESI), *m/z* (M+H)<sup>+</sup>: calcd 343.0747, obsd 343.0762.

**4.3.6. 7-Chloro-2-(2-azidoethyl)anthra[1,9-*cd*]pyrazol-6(2H)-one (7a)**

Mesylate **6a** (2 g, 5.3 mmol) was added to sodium azide (3.0 g, 46 mmol) in DMF (20 mL) and heated to 60 °C under nitrogen for 24 h. The solution was then cooled to room temperature, added to water (200 mL), and stirred for 30 min. The precipitate was filtered, affording **7a** as an orange solid (1.5 g, 87%); mp: 178–179 °C; <sup>1</sup>H NMR (CDCl<sub>3</sub>) δ 8.18–8.24 (m, 1H), 8.03 (dd, *J*<sub>1</sub> = 6.6 Hz, *J*<sub>2</sub> = 1.0 Hz, 1H), 7.66–7.75 (m, 2H), 7.54–7.60 (m, 2H), 4.66 (t, *J* = 5.5 Hz, 2H), 3.93 (t, *J* = 5.5 Hz, 2H); <sup>13</sup>C NMR (CDCl<sub>3</sub>) δ 182.53, 139.61, 139.19, 137.28, 134.44, 133.00, 129.25, 129.08, 127.04, 122.84, 121.93, 121.22, 114.53, 51.08, 49.18; HRMS (ESI), *m/z* (M+H)<sup>+</sup>: calcd 324.0647, obsd 324.0659.

**4.3.7. 2-(2-Azidoethyl)anthra[1,9-*cd*]pyrazol-6(2H)-one (7b)**

Mesylate **6b** (1.88 g, 5.70 mmol) was added to sodium azide (1.86 g, 28.5 mmol) in DMF (10.6 mL) and stirred at room temperature for 2 d. The red-orange reaction mixture was diluted with chloroform and washed with dilute sodium hydroxide. The organic layer was dried over sodium sulfate, condensed, and dried on a vacuum pump to afford the orange solid **7b**: 0.88 g (3.04 mmol, 53%); mp: 176–177 °C; <sup>1</sup>H NMR (CDCl<sub>3</sub>) δ 8.36 (dd, 1H), 8.12 (d, 1H), 7.96 (d, 1H), 7.65 (m, 3H), 7.47 (t, 1H), 4.57 (t, 2H), 3.85 (t, 2H); <sup>13</sup>C NMR (CDCl<sub>3</sub>) δ 183.9, 140.1, 140.0, 133.6, 133.6, 131.8, 129.5, 129.0, 128.9, 126.7, 123.9, 123.0, 121.3, 115.0, 51.34, 49.3; IR (KBr) ν 2103, 1676, 1656, 1595, 1283, 1264, 1033, 998, 773, 701 cm<sup>-1</sup>. HRMS (ESI), *m/z* (M+H)<sup>+</sup>: calcd 290.1036, obsd 290.1047.

**4.3.8. 7-Chloro-2-(2-aminoethyl)anthra[1,9-*cd*]pyrazol-6(2H)-one (8a)**

Azide **7a** (0.5 g, 1.54 mmol) was added to a mixture of methanol (500 mL) and HCl (1.5 mL, 2 M). Palladium on charcoal (0.1 g, 10 wt %) was added and the mixture was stirred under a hydrogen atmosphere for 3 h. The mixture was then filtered through Celite. The filtrate was condensed, extracted into chloroform with dilute sodium hydroxide, dried over sodium sulfate and concentrated to afford **8a** as an orange solid (0.35 g, 76%); mp: 158–160 °C; <sup>1</sup>H NMR (CDCl<sub>3</sub>) δ 8.19–8.22 (m, 1H), 8.00 (d, *J* = 6.9 Hz, 1H), 7.62–7.74 (m, 2H), 7.51–7.58 (m, 2H), 4.57 (t, *J* = 5.9 Hz, 2H), 3.35 (t, *J*<sub>1</sub> = 5.9 Hz, 2H); <sup>13</sup>C NMR (CDCl<sub>3</sub>) δ 181.7, 138.4, 137.4, 136.2, 133.6, 132.0, 131.6, 128.1, 127.7, 125.9, 121.7, 120.8, 120.1, 113.7, 52.1, 41.2; HRMS (ESI), *m/z* (M+H)<sup>+</sup>: calcd 298.0742, obsd 298.0753.

**4.3.9. 2-(2-Aminoethyl)anthra[1,9-*cd*]pyrazol-6(2H)-one (8b)**

Using the same procedure as above, amine **8b** was obtained from **7b** as orange crystals in 62% yield; mp: 178–179 °C; <sup>1</sup>H NMR (CDCl<sub>3</sub>) δ 8.38 (d, 1H), 8.15 (d, 1H), 7.97 (d, 1H), 7.64 (m, 3H), 7.47 (t, 1H), 4.52 (t, 2H), 3.29 (t, 2H); <sup>13</sup>C NMR (CDCl<sub>3</sub>) δ 184.0, 139.8, 139.4, 133.5, 132.0, 129.5, 128.7, 128.6, 126.7, 123.8, 122.9, 121.1, 115.2, 76.4, 53.2, 42.6; IR (KBr) ν 3370, 1655, 1594, 1496, 1396, 1204, 1000, 775, 702 cm<sup>-1</sup>; HRMS (ESI), *m/z* (M+H)<sup>+</sup>: calcd 264.1131, obsd 264.1143.

**4.3.10. 4-[[*(tert*-Butoxyl)carbonyl]amino]-*N*-[2-(7-chloro-6-oxo-6H-dibenzo-[*cd,g*]indazol-2-yl)-ethyl]-1-methylpyrrole-2-carboxamide (9a)**

A solution of 4-*tert*-butoxycarbonylamino-1-methyl-1H-pyrrole-2-carboxylic acid benzotriazol-1-yl ester **10** (393 mg, 1.1 mmol) in dichloromethane (10 mL) was added to a solution of **8a** (300 mg, 1 mmol) in dichloromethane (30 mL). The solution was stirred overnight at room temperature. The reaction mixture was filtered to afford **9a** as a bright orange powder (470 mg, 90%); mp: 243–244 °C; NMR (DMSO-*d*<sub>6</sub>) <sup>1</sup>H δ 9.00 (s, 1H), 8.18 (dd, *J*<sub>1</sub> = 7.6 Hz, *J*<sub>2</sub> = 1.0 Hz, 1H), 8.10 (t, *J* = 6.2 Hz, 1H), 7.99 (d, *J* = 8.2 Hz, 1H), 7.87 (d, *J* = 7.1 Hz, 1H), 7.67–7.76 (m, 2H), 7.61 (dd, *J*<sub>1</sub> = 7.9, *J*<sub>2</sub> = 0.9 Hz, 1H), 6.80 (s, 1H), 6.46 (s, 1H), 4.73 (t, *J* = 5.7 Hz, 2H), 3.69 (m, 2H), 3.65 (s, 3H), 1.42 (s, 9H); <sup>13</sup>C 181.44, 161.46, 152.74, 139.20, 136.93, 135.68, 134.24, 133.84, 132.24, 128.63, 128.06, 125.67, 122.64, 122.22, 121.81, 121.70, 120.45, 116.51, 116.14, 103.38, 78.24, 49.22, 35.65, 28.12; HRMS (ESI), *m/z* (M+H)<sup>+</sup>: calcd 520.1746, obsd 520.1761.

**4.3.11. 4-[[*(tert*-Butoxyl)carbonyl]amino]-*N*-[2-(6-oxo-6H-dibenzo-[*cd,g*]indazol-2-yl)-ethyl]-1-methylpyrrole-2-carboxamide (9b)**

The same procedure as for making **9a** was used. Compound **9b** was obtained from **8b** as a bright orange powder in 87% yield; mp: 242–243 °C; NMR (DMSO-*d*<sub>6</sub>) <sup>1</sup>H 9.00 (s, 1H), 8.30 (d, *J* = 7.7 Hz, 1H), 8.17 (d, *J* = 7.6 Hz, 1H), 8.11 (t, *J* = 5.5 Hz, 1H), 8.01 (d, *J* = 8.2 Hz, 1H), 7.93 (d, *J* = 7.1 Hz, 1H), 7.81 (dt, *J*<sub>1</sub> = 1.0 Hz, *J*<sub>2</sub> = 7.6 Hz, 1H), 7.70 (d, *J* = 7.9 Hz, 1H), 7.61 (dt, *J*<sub>1</sub> = 1.0 Hz, *J*<sub>2</sub> = 7.6 Hz, 1H), 6.80 (s, 1H), 6.47 (s, 1H), 4.74 (t, *J* = 5.7 Hz, 2H), 3.69 (m, 2H), 3.65 (s, 3H), 1.42 (s, 9H); <sup>13</sup>C 182.54, 161.42, 152.71, 139.41, 137.62, 133.73, 132.50, 131.36, 128.60, 128.48, 128.42, 125.16, 122.65, 122.57, 122.48, 122.23, 120.40, 116.52, 116.45, 103.33, 78.20, 49.15, 35.67, 28.14; HRMS (ESI), *m/z* (M+H)<sup>+</sup>: calcd 486.2136, obsd 486.2145.

**4.3.12. 4-Amino-*N*-[2-(7-chloro-6-oxo-6H-dibenzo-[*cd,g*]indazol-2-yl)-ethyl]-1-methylpyrrole-2-carboxamide (11a)**

The cleavage of the *t*-Boc protecting groups on all compounds followed the same procedure. An example is described here. Compound **9a** (200 mg 0.39 mmol) was treated with a mixture of dichloromethane and trifluoroacetic acid (2 mL, ratio 3:1) at room temperature for 2 h. The reaction mixture was concentrated under reduced pressure and the residue was dissolved in water. The solution was then titrated with 1 M aq sodium hydroxide to pH 9, and filtered to afford **11a** as an orange powder (155 mg, 96%); mp: 198–199 °C; NMR (DMSO-*d*<sub>6</sub>) <sup>1</sup>H NMR δ 8.19 (dd, *J*<sub>1</sub> = 7.7 Hz, *J*<sub>2</sub> = 1.3 Hz, 1H), 8.00 (t, *J* = 8.2 Hz, 1H), 7.86–7.90 (m, 2H), 7.64–7.77 (m, 2H), 6.16 (d, *J* = 2 Hz, 1H), 6.00 (d, *J* = 2.0 Hz, 1H), 4.73 (t, *J* = 5.8 Hz, 2H), 3.60–3.80 (m, 4H), 3.58 (s, 3H); <sup>13</sup>C 181.44, 161.60, 139.24, 136.94, 135.70, 134.28, 133.87, 132.26, 131.53, 128.62, 128.10, 125.70, 122.53, 121.80, 121.72, 120.46, 116.20, 113.79, 102.86, 49.32, 35.32; HRMS (ESI), *m/z* (M+H)<sup>+</sup>: calcd 420.1222, obsd 420.1229.

**4.3.13. 4-Amino-*N*-[2-(6-oxo-6H-dibenzo-[*cd,g*]indazol-2-yl)-ethyl]-1-methylpyrrole-2-carboxamide (11b)**

Compound **11b** was obtained from **9b** in 91% yield as an orange powder; mp: 153–155 °C; NMR (DMSO-*d*<sub>6</sub>) <sup>1</sup>H NMR δ 8.31 (dd, *J*<sub>1</sub> = 8.0 Hz, *J*<sub>2</sub> = 1.0 Hz, 1H), 8.18 (dd, *J*<sub>1</sub> = 7.8 Hz, *J*<sub>2</sub> = 0.7 Hz, 1H), 8.03 (d, *J* = 8.2 Hz, 1H), 7.94 (d, *J* = 7.1 Hz, 1H), 7.89 (t, *J* = 5.8 Hz, 1H), 7.83 (dt, *J*<sub>1</sub> = 1.3 Hz, *J*<sub>2</sub> = 7.5 Hz, 1H), 7.69–7.74 (m, 1H), 7.62 (dt, *J*<sub>1</sub> = 1.3 Hz, *J*<sub>2</sub> = 7.7 Hz, 1H), 6.16 (d, *J* = 2.0 Hz, 1H), 5.99 (d, *J* = 2.0 Hz, 1H), 4.73 (t, *J* = 5.8 Hz, 2H), 3.62–3.86 (m, 4H), 3.59 (s, 3H); <sup>13</sup>C 182.57, 161.60, 139.44, 137.62, 133.77, 132.51, 131.52, 131.37, 128.62, 128.48, 128.45, 125.18, 122.58, 122.54, 122.47,

120.43, 116.58, 113.75, 102.83, 49.24, 35.31; HRMS (ESI),  $m/z$  (M+H)<sup>+</sup>: calcd 386.1612, obsd 386.1619.

**4.3.14. 4-[[2-(Dimethylamino)acetyl]amino]-N-[2-(7-chloro-6-oxo-6H-dibenzo-[cd,g]indazol-2-yl)-ethyl]-1-methylpyrrole-2-carboxamide (12a)**

To a stirred solution of compound **11a** (50 mg, 0.12 mmol), anhydrous triethylamine (95  $\mu$ L, 0.63 mmol) and DMF (dried, 2 mL) was added dimethylaminoacetyl chloride hydrochloride (39 mg, 0.24 mmol). The mixture was stirred at room temperature for 3 h and then poured into 30 mL of ice-water. The precipitate formed was filtered to afford **12a** as a brown powder (50 mg, 83%); mp: 160–162 °C; NMR (DMSO- $d_6$ ) <sup>1</sup>H NMR  $\delta$  9.57 (s, 1H), 8.13–8.16 (m, 2H), 7.97 (d,  $J$  = 8.3 Hz, 1H), 7.84 (d,  $J$  = 6.9 Hz, 1H), 7.65–7.63 (m, 2H), 7.60 (d,  $J$  = 7.8 Hz, 1H), 7.09 (s, 1H), 6.63 (s, 1H), 4.73 (t,  $J$  = 5.8 Hz, 2H), 3.66–3.71 (m, 5H), 3.32 (s, 2H), 2.23 (s, 6H); <sup>13</sup>C 181.48, 161.65, 161.45, 139.27, 136.99, 135.71, 134.30, 133.91, 132.29, 128.69, 128.13, 125.73, 122.63, 121.86, 121.77, 121.48, 117.80, 116.22, 104.00, 69.69, 49.24, 45.24, 35.71; HRMS (ESI),  $m/z$  (M+H)<sup>+</sup>: calcd 505.1749, obsd 505.1761.

**4.3.15. 4-[[2-(Dimethylamino)acetyl]amino]-N-[2-(6-oxo-6H-dibenzo-[cd,g]indazol-2-yl)-ethyl]-1-methylpyrrole-2-carboxamide (12b)**

The same procedure as for preparing **12a** was used. Compound **12b** was prepared from **11b** to give a brown solid in 80% yield; mp: 145–146 °C; NMR (DMSO- $d_6$ ) <sup>1</sup>H NMR  $\delta$  9.59 (s, 1H), 8.31 (dd,  $J_1$  = 7.9 Hz,  $J_2$  = 0.9 Hz, 1H), 8.18 (dd,  $J_1$  = 7.9 Hz,  $J_2$  = 0.9 Hz, 1H), 8.14 (t,  $J$  = 6 Hz, 1H), 8.03 (d,  $J$  = 8.2 Hz, 1H), 7.94 (d,  $J$  = 7.0 Hz, 1H), 7.62–7.85 (m, 3H), 7.08 (d,  $J$  = 1.8 Hz, 1H), 6.63 (d,  $J$  = 1.8 Hz, 1H), 4.76 (t,  $J$  = 5.8 Hz, 2H), 3.66–3.73 (m, 5H), 3.00 (s, 2H), 2.23 (s, 6H); <sup>13</sup>C 182.57, 161.47, 139.45, 137.65, 133.78, 132.52, 131.37, 128.63, 128.52, 128.47, 125.19, 122.65, 122.60, 121.47, 120.45, 117.79, 116.58, 103.98, 62.68, 49.14, 45.24, 35.71; HRMS (ESI),  $m/z$  (M+H)<sup>+</sup>: calcd 471.2139, obsd 471.2151.

**4.3.16. 4-[[4-[[2-(Dimethylamino)acetyl]amino]-1-methyl-2-pyrrolyl]carbonyl]amino]-N-[2-(7-chloro-6-oxo-6H-dibenzo-[cd,g]indazol-2-yl)-ethyl]-1-methylpyrrole-2-carboxamide (13a)**

The same procedure as for preparing **9a** was used. Compound **13a** was prepared from **11a** to afford a brown powder in 87% yield; mp: 226–228 °C; NMR (DMSO- $d_6$ ) <sup>1</sup>H  $\delta$  9.77 (s, 1H), 9.07 (s, 1H), 8.14–8.18 (m, 2H), 7.98 (d,  $J$  = 8.2 Hz, 1H), 7.88 (d,  $J$  = 7.1 Hz, 1H), 7.66–7.74 (m, 2H), 7.59 (d,  $J$  = 7.8 Hz, 1H), 7.13 (s, 1H), 6.87 (s, 1H), 6.79 (s, 1H), 6.73 (s, 1H), 4.74 (t,  $J$  = 5.2 Hz, 2H), 3.68–3.78 (m, 8H), 1.45 (s, 9H); <sup>13</sup>C 181.48, 161.53, 158.31, 152.81, 139.27, 136.98, 135.71, 134.31, 133.90, 132.29, 128.70, 128.13, 125.74, 122.76, 122.50, 122.14, 121.88, 121.77, 120.51, 117.92, 116.96, 116.22, 104.30, 103.73, 78.23, 49.27, 35.97, 35.74, 28.17; HRMS (ESI),  $m/z$  (M+H)<sup>+</sup>: calcd 642.2226, obsd 642.2241.

**4.3.17. 4-[[4-[[2-(Dimethylamino)acetyl]amino]-1-methyl-2-pyrrolyl]carbonyl]amino]-N-[2-(6-oxo-6H-dibenzo-[cd,g]indazol-2-yl)-ethyl]-1-methylpyrrole-2-carboxamide (13b)**

The same procedure as for preparing **9a** was used. Compound **13b** was prepared from **11b** and gave a bright orange powder in 82% yield; mp: 234–235 °C; NMR (DMSO- $d_6$ ) <sup>1</sup>H  $\delta$  9.77 (s, 1H), 9.07 (s, 1H), 8.31 (d,  $J$  = 7.8 Hz, 1H), 8.14–8.20 (m, 2H), 8.03 (d,  $J$  = 8.2 Hz, 1H), 7.94 (d,  $J$  = 7.1 Hz, 1H), 7.81 (t,  $J$  = 7.3 Hz, 1H), 7.72 (t,  $J$  = 7.8 Hz, 1H), 7.61 (t,  $J$  = 7.5 Hz, 1H), 7.13 (s, 1H), 6.87 (s, 1H), 6.78 (s, 1H), 6.73 (s, 1H), 4.78 (t,  $J$  = 5.2 Hz, 2H), 3.68–3.78 (m, 8H), 1.45 (s, 9H); <sup>13</sup>C 182.56, 161.54, 158.30, 152.81, 139.42, 137.63, 133.75, 132.51, 131.36, 128.61, 128.52, 125.18, 122.76, 122.58, 122.51, 122.24, 122.13, 120.44, 117.91, 116.96, 116.54,

104.28, 103.71, 78.23, 49.17, 35.97, 35.73, 28.17; HRMS (ESI),  $m/z$  (M+H)<sup>+</sup>: calcd 608.2616, obsd 608.2629.

**4.3.18. 4-[[4-[(4-Amino-1-methyl-2-pyrrolyl)carbonyl]amino]-N-[2-(7-chloro-6-oxo-6H-dibenzo-[cd,g]indazol-2-yl)-ethyl]-1-methylpyrrole-2-carboxamide (14a)**

The same deprotection procedure as for **11a** was used. Compound **14a** was obtained from **13a** as a light brown powder in 93% yield; mp: 182–184 °C; NMR (DMSO- $d_6$ ) <sup>1</sup>H NMR  $\delta$  9.52 (s, 1H), 8.19 (dd,  $J_1$  = 7.6 Hz,  $J_2$  = 1.0 Hz, 1H), 8.15 (t,  $J$  = 5.6 Hz, 1H), 8.01 (d,  $J$  = 8.2 Hz, 1H), 7.88 (d,  $J$  = 7.1 Hz, 1H), 7.69–7.74 (m, 2H), 7.61 (dd,  $J_1$  = 7.9 Hz,  $J_2$  = 0.9 Hz, 1H), 7.11 (d,  $J$  = 1.5 Hz, 1H), 6.69 (d,  $J$  = 1.6 Hz, 1H), 6.32 (d,  $J$  = 1.9 Hz, 1H), 6.24 (d,  $J$  = 1.9 Hz, 1H), 4.76 (t,  $J$  = 5.6 Hz, 2H), 3.81 (s, br, 2H), 3.68–3.70 (m, 8H); <sup>13</sup>C 181.54, 161.54, 158.49, 139.32, 137.02, 135.74, 134.35, 133.97, 132.33, 131.60, 128.75, 128.18, 125.78, 122.60, 122.43, 122.27, 121.91, 121.81, 120.55, 117.83, 116.30, 114.15, 104.22, 103.15, 49.30, 35.73, 35.56; HRMS (ESI),  $m/z$  (M+H)<sup>+</sup>: calcd 542.1702, obsd 542.1715.

**4.3.19. 4-[[4-[(4-Amino-1-methyl-2-pyrrolyl)carbonyl]amino]-N-[2-(6-oxo-6H-dibenzo-[cd,g]indazol-2-yl)-ethyl]-1-methylpyrrole-2-carboxamide (14b)**

The same deprotection procedure as for **11a** was used. Compound **14b** was obtained from **13b** as a light brown powder in 90% yield; mp: 188–189 °C; NMR (DMSO- $d_6$ ) <sup>1</sup>H  $\delta$  9.53 (s, 1H), 8.29 (d,  $J$  = 7.6 Hz, 1H), 8.14–8.18 (m, 2H), 8.01 (d,  $J$  = 7.8 Hz, 1H), 7.92 (d,  $J$  = 7.1 Hz, 1H), 7.80 (t,  $J$  = 7.8 Hz, 1H), 7.70 (t,  $J$  = 8.0 Hz, 1H), 7.60 (t,  $J$  = 7.6 Hz, 1H), 7.12 (s, 1H), 6.69 (s, 1H), 6.33 (s, 1H), 6.25 (s, 1H), 4.75 (t,  $J$  = 5.2 Hz, 2H), 3.68–3.86 (m, 8H); <sup>13</sup>C 182.54, 161.55, 158.50, 139.39, 137.60, 133.71, 132.48, 131.59, 131.34, 128.58, 128.48, 128.41, 125.16, 122.61, 122.56, 122.48, 122.45, 122.27, 120.40, 117.84, 116.49, 114.18, 104.21, 103.17, 49.15, 35.72, 35.56; HRMS (ESI),  $m/z$  (M+H)<sup>+</sup>: calcd 508.2092, obsd 508.2100.

**4.3.20. 4-[[4-[[2-(Dimethylamino)acetyl]amino]-1-methyl-2-pyrrolyl]carbonyl]amino]-N-[2-(7-chloro-6-oxo-6H-dibenzo-[cd,g]indazol-2-yl)-ethyl]-1-methylpyrrole-2-carboxamide (15a)**

The same procedure as for **12a** was used. Compound **15a** was prepared from **14a** as a brown powder in 89% yield; mp: 186–187 °C; NMR (DMSO- $d_6$ ) <sup>1</sup>H  $\delta$  9.81 (s, 1H), 9.66 (s, 1H), 8.14–8.20 (m, 2H), 8.00 (d,  $J$  = 8.2 Hz, 1H), 7.87 (d,  $J$  = 7.1 Hz, 1H), 7.68–7.75 (m, 2H), 7.61 (d,  $J$  = 7.2 Hz, 1H), 7.16 (d,  $J$  = 1.4 Hz, 1H), 7.14 (d,  $J$  = 1.2 Hz, 1H), 6.93 (d,  $J$  = 1.5 Hz, 1H), 6.71 (d,  $J$  = 1.4 Hz, 1H), 4.75 (t,  $J$  = 5.4 Hz, 2H), 3.69–3.80 (m, 8H), 3.01 (s, 2H), 2.25 (s, 6H); <sup>13</sup>C 181.52, 166.81, 161.52, 158.33, 139.31, 136.98, 137.00, 134.31, 135.73, 134.34, 133.95, 132.32, 128.74, 128.16, 125.77, 122.77, 122.52, 122.07, 121.90, 121.80, 121.49, 120.54, 118.19, 117.96, 116.27, 104.37, 104.26, 62.80, 49.29, 49.28, 45.30, 35.97, 35.75; HRMS (ESI),  $m/z$  (M+H)<sup>+</sup>: calcd 627.2230, obsd 627.2239.

**4.3.21. 4-[[4-[[2-(Dimethylamino)acetyl]amino]-1-methyl-2-pyrrolyl]carbonyl]amino]-N-[2-(6-oxo-6H-dibenzo-[cd,g]indazol-2-yl)-ethyl]-1-methylpyrrole-2-carboxamide (15b)**

The same procedure as for making **12a** was used. Compound **15b** was prepared from **14b** in 83% yield as a brown powder; mp: 176–178 °C; NMR (DMSO- $d_6$ ) <sup>1</sup>H  $\delta$  9.53 (s, 1H), 8.29 (d,  $J$  = 7.6 Hz, 1H), 8.14–8.18 (m, 2H), 8.01 (d,  $J$  = 7.8 Hz, 1H), 7.92 (d,  $J$  = 7.1 Hz, 1H), 7.80 (t,  $J$  = 7.8 Hz, 1H), 7.70 (t,  $J$  = 8.0 Hz, 1H), 7.60 (t,  $J$  = 7.6 Hz, 1H), 7.12 (s, 1H), 6.69 (s, 1H), 6.33 (s, 1H), 6.25 (s, 1H), 4.75 (t,  $J$  = 5.2 Hz, 2H), 3.68–3.86 (m, 8H); <sup>13</sup>C 182.55, 166.87, 161.53, 158.34, 139.42, 137.62, 133.74, 132.50, 131.36, 128.60, 128.50, 128.43, 125.18, 122.77, 122.58, 122.54, 122.49, 122.08, 121.51, 120.42, 118.19, 117.97, 116.51, 104.38, 104.25, 62.87,

49.16, 45.32, 35.97, 35.76; HRMS (ESI),  $m/z$  (M+H)<sup>+</sup>: calcd 593.2619, obsd 593.2633.

**4.3.22. 4-[[4-[[2-(Dimethylamino)acetyl]amino]-1-methyl-2-pyrrolyl]carbonyl] amino)-N-[2-(7-[[2-(dimethylamino)ethyl]amino]-6-oxo-6H-dibenzo-[c,d,g]indazol-2-yl)-ethyl]-1-methylpyrrole-2-carboxamide (16)**

Compound **15a** (63 mg, 0.1 mmol) was treated with *N*<sup>1</sup>,*N*<sup>1</sup>-dimethylethane-1,2-diamine (0.1 mL, 0.92 mmol) in DMSO (1 mL) at 100 °C overnight under nitrogen. After the reaction mixture was cooled, 10 mL water was added and the product was extracted into dichloromethane. The dichloromethane layer was then washed with water (10 mL × 5) and dried over Na<sub>2</sub>SO<sub>4</sub>. The solvent was removed under reduced pressure. The red residue was then purified on a silica gel column using ethyl acetate/methanol/triethylamine (3:1:1, v/v/v) as eluant, affording **16** as a red powder (14 mg, 20%); mp: 166–167 °C; NMR (CDCl<sub>3</sub>) 10.15 (s, 1H), <sup>1</sup>H δ 9.81 (s, 1H), 9.66 (s, 1H), 8.14–8.20 (m, 2H), 8.00 (d, *J* = 8.2 Hz, 1H), 7.87 (d, *J* = 7.1 Hz, 1H), 7.68–7.75 (m, 2H), 7.61 (d, *J* = 7.2, 1H), 7.16 (d, *J* = 1.4 Hz, 1H), 7.14 (d, *J* = 1.2 Hz, 1H), 6.93 (d, *J* = 1.5 Hz, 1H), 6.71 (d, *J* = 1.4 Hz, 1H), 4.75 (t, *J* = 5.4 Hz, 2H), 3.69–3.80 (m, 8H), 3.01 (s, 2H), 2.69 (d, *J* = 6.6 Hz, 2H), 2.36 (s, 6H), 2.25 (s, 6H); <sup>13</sup>C; HRMS (ESI),  $m/z$  (M+H)<sup>+</sup>: calcd 679.3463, obsd 679.3471.

## Acknowledgments

Supported by grants from the Canadian Institutes of Health Research, the Canada Research Chairs Program, a Canada Research Chair in Drug Development to Brian Hasinoff, the Robert A. Welch Foundation (Grant AF-0005), the Herbert and Kate Dishman Endowment at Southwestern University to Frank Guziec and NIH grant CA90787 to Jack Yalowich.

## Supplementary data

Supplementary data associated with this article can be found, in the online version, at doi:10.1016/j.bmc.2010.04.028.

## References and notes

- Corbett, A. H.; Osheroff, N. *Chem. Res. Toxicol.* **1993**, *6*, 585.
- Malisza, K. L.; Hasinoff, B. B. *Arch. Biochem. Biophys.* **1995**, *321*, 51.
- Leteurtre, F.; Kohlhaagen, G.; Paul, K. D.; Pommier, Y. *J. Natl. Cancer Inst.* **1994**, *86*, 1239.
- Capranico, G.; Palumbo, M.; Tinelli, S.; Mabilia, M.; Pozzan, A.; Zunino, F. *J. Mol. Biol.* **1994**, *28*, 1218.
- Liang, H.; Wu, X.; Guziec, L. J.; Guziec, F. S., Jr.; Larson, K. K.; Lang, J.; Yalowich, J. C.; Hasinoff, B. B. *J. Chem. Inf. Model.* **2006**, *46*, 1827.
- Hasinoff, B. B.; Liang, H.; Wu, X.; Guziec, L. J.; Guziec, F. S., Jr.; Yalowich, J. C. *Bioorg. Med. Chem.* **2008**, *16*, 3959.
- Hasinoff, B. B.; Zhang, R.; Wu, X.; Guziec, L. J.; Guziec, F. S., Jr.; Marshall, K.; Yalowich, J. C. *Bioorg. Med. Chem.* **2009**, *17*, 4575.
- Bailly, C.; Chaires, J. B. *Bioconj. Chem.* **1998**, *9*, 513.
- Bourdouxhe, C.; Colson, P.; Houssier, C.; Henichart, J. P.; Waring, M. J.; Denny, W. A.; Bailly, C. *Anticancer Drug Des.* **1995**, *10*, 131.
- Bourdouxhe-Housiaux, C.; Colson, P.; Houssier, C.; Waring, M. J.; Bailly, C. *Biochemistry* **1996**, *35*, 4251.
- David-Cordonnier, M. H.; Hildebrand, M. P.; Baldeyrou, B.; Lansiaux, A.; Keuser, C.; Benzschawel, K.; Lemster, T.; Pindur, U. *Eur. J. Med. Chem.* **2007**, *42*, 752.
- Pindur, U.; Jansen, M.; Lemster, T. *Curr. Med. Chem.* **2005**, *12*, 2805.
- Carrasco, C.; Helissey, P.; Haroun, M.; Baldeyrou, B.; Lansiaux, A.; Colson, P.; Houssier, C.; Giorgi-Renault, S.; Bailly, C. *ChemBioChem* **2003**, *4*, 50.
- Liang, H.; Wu, X.; Yalowich, J. C.; Hasinoff, B. B. *Mol. Pharmacol.* **2008**, *73*, 686.
- Pommier, Y.; Pourquier, P.; Fan, Y.; Strumberg, D. *Biochim. Biophys. Acta* **1998**, *1400*, 83.
- Fortune, J. M.; Osheroff, N. *Prog. Nucl. Acid Res. Mol. Biol.* **2000**, *64*, 221.
- Li, T. K.; Liu, L. F. *Annu. Rev. Pharmacol. Toxicol.* **2001**, *41*, 53.
- Hasinoff, B. B.; Kozłowska, H.; Creighton, A. M.; Allan, W. P.; Thampatty, P.; Yalowich, J. C. *Mol. Pharmacol.* **1997**, *52*, 839.
- Burden, D. A.; Froelich-Ammon, S. J.; Osheroff, N. *Methods Mol. Biol.* **2001**, *95*, 283.
- Hasinoff, B. B.; Wu, X.; Begleiter, A.; Guziec, L.; Guziec, F. S., Jr.; Giorgianni, A.; Yang, S.; Jiang, Y.; Yalowich, J. C. *Cancer Chemother. Pharmacol.* **2006**, *57*, 221.
- Orłowski, S.; Belehradek, J., Jr.; Paoletti, C.; Mir, L. M. *Biochem. Pharmacol.* **1988**, *37*, 4727.
- Fattman, C.; Allan, W. P.; Hasinoff, B. B.; Yalowich, J. C. *Biochem. Pharmacol.* **1996**, *52*, 635.
- Ritke, M. K.; Allan, W. P.; Fattman, C.; Gunduz, N. N.; Yalowich, J. C. *Mol. Pharmacol.* **1994**, *46*, 58.
- Ritke, M. K.; Roberts, D.; Allan, W. P.; Raymond, J.; Bergoltz, V. V.; Yalowich, J. C. *Br. J. Cancer* **1994**, *69*, 687.
- Leonard, G. A.; Hambley, T. W.; McAuley-Hecht, K.; Brown, T.; Hunter, W. N. *Acta Crystallogr., Sect. D* **1993**, *49*, 458.
- Balendiran, K.; Rao, S. T.; Sekharudu, C. Y.; Zon, G.; Sundaralingam, M. *Acta Crystallogr., Sect. D* **1995**, *51*, 190.
- Bailly, C.; Pommery, N.; Houssin, R.; Henichart, J. P. *J. Pharm. Sci.* **1989**, *78*, 910.
- Rene, B.; Fosse, P.; Khelifa, T.; Jacquemin-Sablon, A.; Bailly, C. *Mol. Pharmacol.* **1996**, *49*, 343.
- Boitte, N.; Pommery, N.; Colson, P.; Houssier, C.; Waring, M. J.; Henichart, J. P.; Bailly, C. *Anticancer Drug Des.* **1997**, *12*, 481.
- Hasinoff, B. B.; Wu, X.; Krokhin, O. V.; Ens, W.; Standing, K. G.; Nitiss, J. L.; Sivaram, T.; Giorgianni, A.; Yang, S.; Jiang, Y.; Yalowich, J. C. *Mol. Pharmacol.* **2005**, *67*, 937.
- Hasinoff, B. B.; Kuschak, T. I.; Creighton, A. M.; Fattman, C. L.; Allan, W. P.; Thampatty, P.; Yalowich, J. C. *Biochem. Pharmacol.* **1997**, *53*, 1843.
- Sissi, C.; Leo, E.; Moro, S.; Capranico, G.; Mancina, A.; Menta, E.; Krapcho, A. P.; Palumbo, M. *Biochem. Pharmacol.* **2004**, *67*, 631.
- Priebe, W.; Fokt, I.; Przewłoka, T.; Chaires, J. B.; Portugal, J.; Trent, J. O. *Methods Enzymol.* **2001**, *340*, 529.
- McGhee, J. D. *Biopolymers* **1976**, *15*, 1345.
- GOLD 3.2, CCDC Software Ltd, Cambridge, UK.
- SYBYL 7.3, Tripos Inc., 1699 South Hanley Rd., St. Louis, MO, 63144, USA.
- Verdonk, M. L.; Cole, J. C.; Hartshorn, M. J.; Murray, C. W.; Taylor, R. D. *Proteins* **2003**, *52*, 609.